

**Aquatic photochemical kinetics of benzotriazole and structurally related
compounds**

Elisabeth M.L. Janssen, Emily Marron, Kristopher McNeill*

Institute of Biogeochemistry and Pollutant Dynamics, ETH Zurich,
CH-8092, Zurich, Switzerland

Supporting Information

The supporting information contains 16 pages numbered S1-S16, 8 figures, 4 table.

Content

		page
Light spectra	Figure S1	S3
Formation of hydroxyterephthalic acid	Figure S2	S4
Degradation in enhanced UVB light	Figure S3	S5
Quantum yield calculations		S6
	Table S1	S7
	Table S2	S8
Reaction with hydroxyl radicals	Figure S4	S9
	Figure S5	S10
Product formation	Figure S6	S11
Chromatograms	Figure S7	S12
Decay in simulated sunlight	Figure S8	S13
Reaction with singlet oxygen	Table S3	S14
Light screening correction	Table S4	S15
References		S16

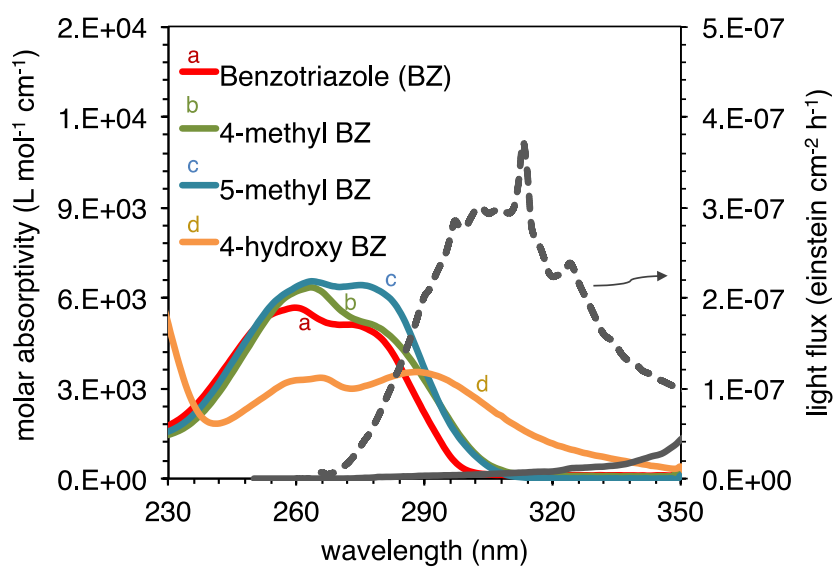


Figure S1. Light flux of simulated sunlight (Xe-lamp, grey solid line) and enhanced UVB light (Rayonet reactor with six light bulbs, grey dashed line) and molar absorptivities and chemical structures of benzotriazole and its derivatives.

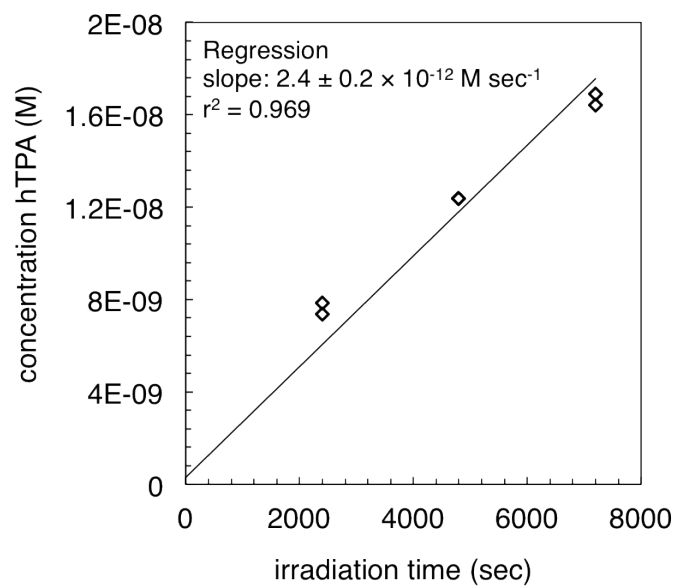


Figure S2. Formation of hydroxyterephthalic acid (hTPA) during the irradiation of TPA with simulated sunlight in the presence of dissolved organic matter (Suwannee River Fulvic Acid (II), $13 \text{ mg}_C \text{ L}^{-1}$). Measurements were performed in duplicate.

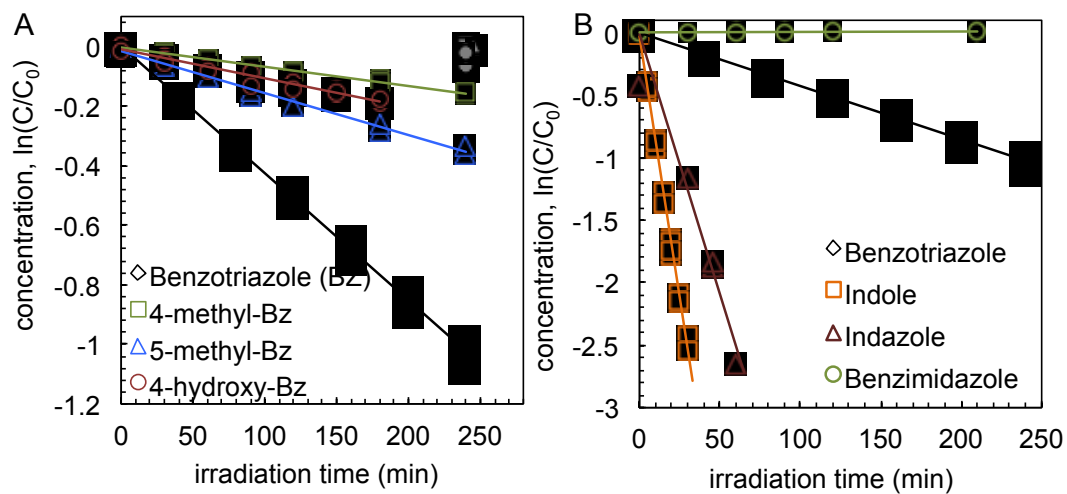


Figure S3. Degradation during exposure to enhanced UVB light for (A) benzotriazole derivatives 4-methylbenzotriazole (green squares), 5-methylbenzotriazole (blue triangles) and 4-hydroxybenzotriazole (red circles) and, (B) benzimidazole (green circles), benzotriazole (black diamonds), indazole (red triangles), and indole (orange squares). Dark control samples are shown in grey symbols. Measurements were performed in duplicates.

Quantum yield calculations

The irradiance, I_λ , of the enhanced UVB light was recorded with a spectrometer (OceanOptics Inc.) and the spectral flux, $\Sigma(I_\lambda \cdot \varepsilon_\lambda)$ ($\text{Es mol}^{-1} \text{s}^{-1}$) was calculated as the sum of I_λ and the molar absorptivity of the test compounds, ε_λ □ □:

$$\sum_{\lambda=270\text{nm}}^n (I_\lambda \cdot \varepsilon_\lambda)$$

The spectral range of 270 nm to 310 nm was used for all test compounds except for 4-hydroxybenzotriazole, where the range was extended to 360 nm.

Then the quantum yield for the test compound, ϕ_i (mol Es^{-1}) is calculated relative to the actinometer para-nitroanisole (PNA) as:

$$\phi_i = \frac{\Sigma(I_\lambda \cdot \varepsilon_\lambda)_{PNA} \cdot k_i}{k_{PNA} \cdot \Sigma(I_\lambda \cdot \varepsilon_\lambda)_i} \cdot \phi_{PNA}$$

The quantum yield of PNA, ϕ_{PNA} , was calculated for a pyridine concentration, [PYR], of 0.5 mM as described elsewhere (Dulin and Mill 1982):

$$\phi_{PNA} = 0.437 \cdot [\text{PYR}] + 0.000282 = 4.39 \cdot 10^{-4}$$

Table S1. Observed degradation rates, spectral flux and quantum yields for direct photochemical degradation calculated from experimental data using enhanced UVB light. The observed degradation rate of para-nitroanisole was $2.88 \times 10^{-4} \text{ s}^{-1}$.

	Observed degradation rate constant, k (\pm stdev) (s^{-1})	r^2	Quantum yield ϕ (mol Es^{-1})
Benzotriazole (BZ)	7.11 $\pm 0.10 \times 10^{-5}$	0.995	0.0022
5-methyl BZ	2.35 $\pm 0.05 \times 10^{-5}$	0.990	0.0037
4-methyl BZ	1.07 $\pm 0.02 \times 10^{-5}$	0.993	0.0018
4-hydroxy BZ	1.62 $\pm 0.06 \times 10^{-5}$	0.968	0.0016
Indole	1.39 $\pm 0.02 \times 10^{-3}$	0.995	0.049
Indazole	7.27 $\pm 0.03 \times 10^{-4}$	0.999	0.012
Benzimidazole	n.d.	n.d.	n.d.

Table S2. Observed degradation rates, spectral flux and quantum yields for direct photochemical degradation calculated from experimental data using a solar simulator (Xe-lamp). The observed degradation rate of para-nitroanisole was $3.67 \times 10^{-5} \text{ s}^{-1}$.

	Observed degradation rate constant, k (\pm stdev) (s^{-1})	r^2	Quantum yield ϕ (mol Es^{-1})
Benzotriazole (BZ)	4.98 $\pm 0.24 \times 10^{-6}$	0.978	0.0044
5-methyl BZ	5.67 $\pm 0.45 \times 10^{-6}$	0.918	0.0026
4-methyl BZ	5.04 $\pm 0.61 \times 10^{-6}$	0.933	0.0025
4-hydroxy BZ	6.18 $\pm 0.49 \times 10^{-6}$	0.929	0.0018
Indole	8.80 $\pm 0.20 \times 10^{-5}$	0.997	0.088
Indazole	2.87 $\pm 0.03 \times 10^{-5}$	0.999	0.015
Benzimidazole	n.d.	n.d.	n.d.

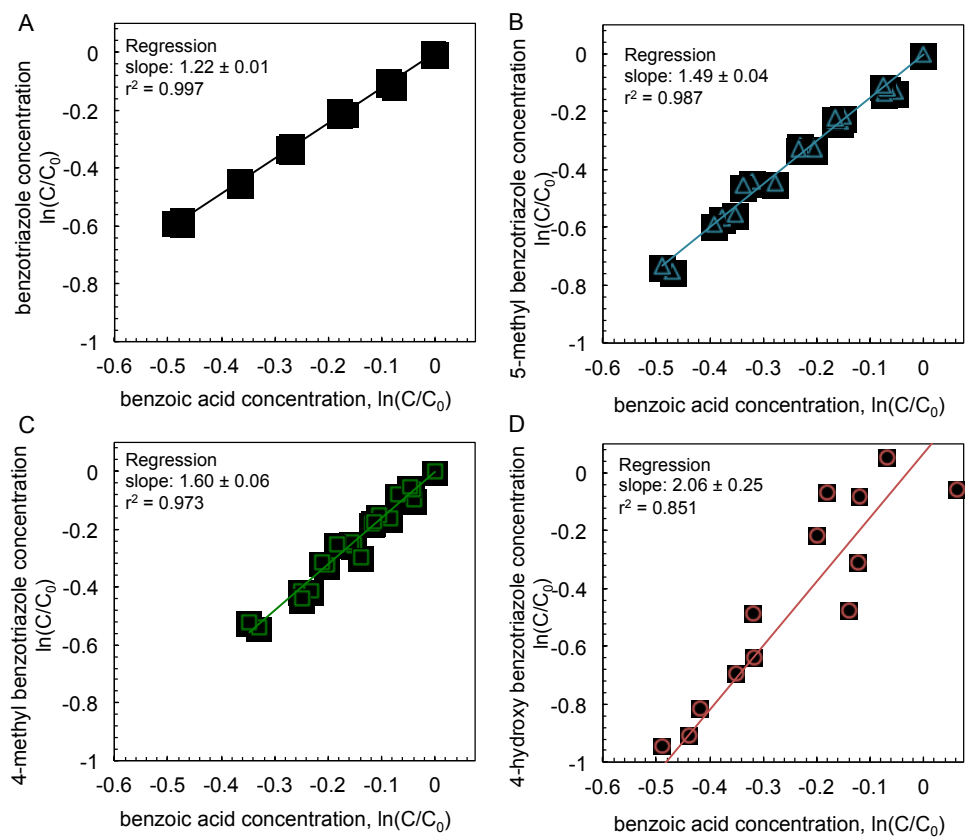


Figure S4. Degradation by hydroxyl radical relative to the degradation of benzoic acid for (A) benzotriazole, (B) 5-methylbenzotriazole, (C) 4-methylbenzotriazole, and (D) 4-hydroxybenzotriazole. Measurements were performed in triplicate.

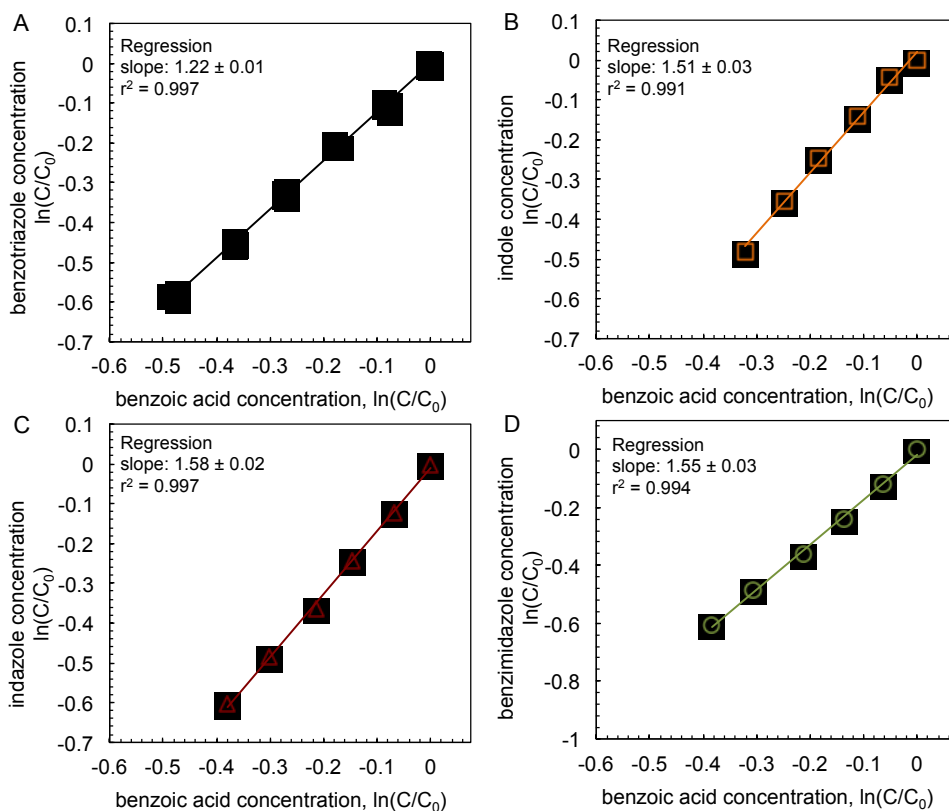


Figure S5. Degradation by hydroxyl radical relative to the degradation of benzoic acid for (A) benzotriazole, (B) indole, (C) indazole, and (D) benzimidazole. Measurements were performed in duplicate or triplicate.

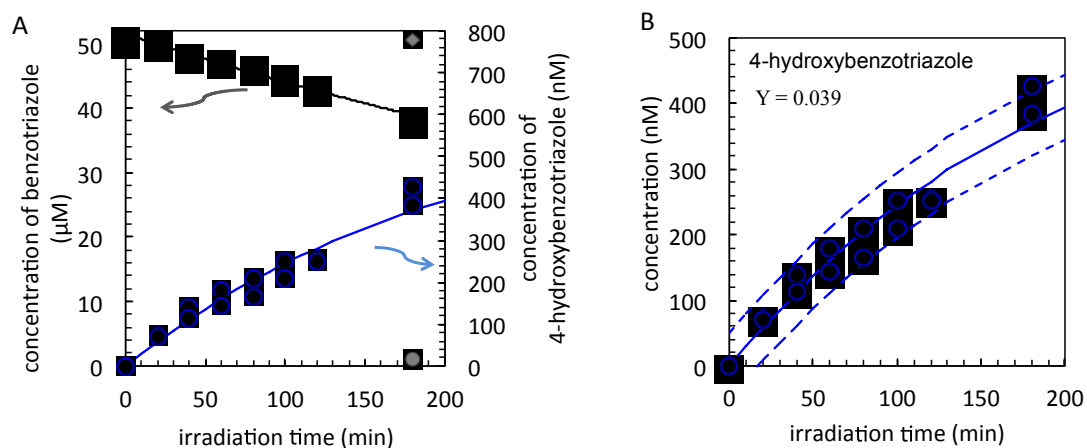
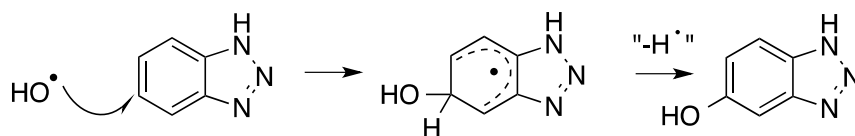


Figure S6. Benzotriazole degradation was followed in the presence of hydroxyl radical. Hydroxyl radicals were generated by irradiation of hydrogen peroxide with UVA light. (A) Decreasing concentration of benzotriazole (black diamonds, in μM , lines represent modeled exponential decay), and formation of 4-hydroxybenzotriazole (blue circles, in nM, lines represent modeled product formation considering its simultaneous reaction with hydroxyl radical, see rate constant in Table1). (B) Formation of 4-hydroxybenzotriazole from the reaction of benzotriazole with hydroxyl radical had a yield (Y) of 3.9%. Solid lines show the modeled concentrations and dashed lines represent the 95% confidence intervals of the model.

Proposed reaction mechanism of hydroxyl radical with benzotriazole:



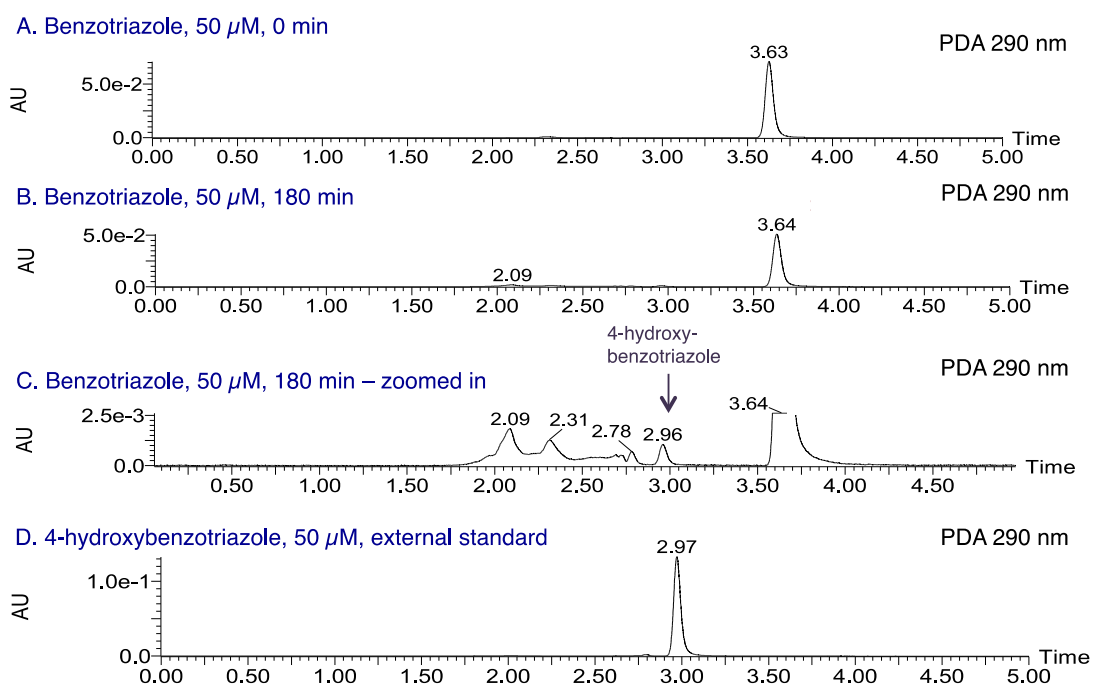


Figure S7. Chromatograms for absorbance detection at 290 nm for (A) 50 μ M benzotriazole solution before irradiation and (B) after 180 minutes exposure to hydroxyl radicals (corresponding to data in Figure S6), (C) Zoomed-in chromatogram (B) showing low intensity peaks between two and three minutes retention time, and (D) 50 μ M standard solution of 4-hydroxybenzotriazole.

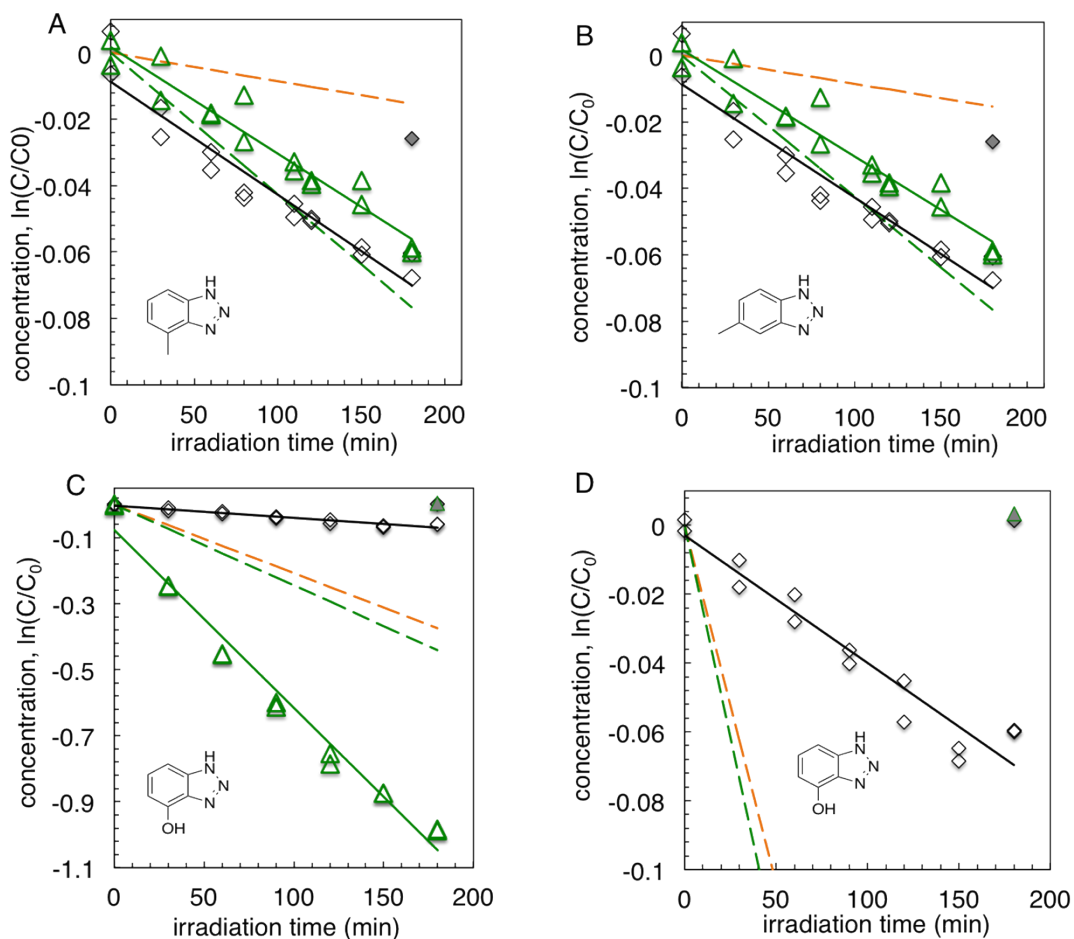


Figure S8. Degradation during exposure to simulated sunlight (black diamonds) and in the presence of organic matter (green triangles, Suwannee River Fulvic Acid (II), 13 mg_C L⁻¹, corrected for light screening). Solid lines represent linear regression of measured data, dashed lines represent estimates for the reaction with hydroxyl radical and singlet oxygen (orange line) and the sum of direct and indirect reactions in the presence of organic matter (green line) for (A) 4-methylbenzotriazole, (B) 5-methylbenzotriazole, (C) 4-hydroxybenzotriazole, and (D) enlargement of the data in (C) and dark controls (grey symbols). Measurements were performed in duplicates.

Table S3. Reaction rate constants of test compounds with singlet oxygen for experiments with Rose Bengal as a sensitizer and irradiation with > 455 nm light from a Xe-lamp. Presented are the concentration of Rose Bengal (μM), the observed decay rate constant of the singlet oxygen probe molecule furfuryl alcohol ($k_{(\text{FFA})}$, s^{-1}), the estimated steady-state singlet oxygen concentration ($[^1\text{O}_2]_{\text{ss}}$, M), the observed decay rate constant of the test compound ($k_{(\text{obs})}$, s^{-1}) and the reaction rate constant of the test compound with singlet oxygen ($k_{(\text{rxn})}$, $\text{M}^{-1} \text{s}^{-1}$).

Rose Bengal (μM)	$k_{(\text{FFA})}$ (s^{-1})	$[^1\text{O}_2]_{\text{ss}}$ (M)	Test compound	$k_{(\text{obs})}$ (s^{-1})	$k_{(\text{rxn})}$ ($\text{M}^{-1} \text{s}^{-1}$)
10	7.00 $\pm 0.20 \times 10^{-3}$	8.43 $\pm 0.26 \times 10^{-11}$	Benzotriazole (BZ)	1.13 $\pm 0.14 \times 10^{-5}$	$< 2.0 \times 10^5$
10	6.36 $\pm 0.04 \times 10^{-3}$	7.67 $\pm 0.11 \times 10^{-11}$	5-methyl BZ	4.80 $\pm 0.22 \times 10^{-6}$	$< 6.2 \times 10^4$
10	7.43 $\pm 0.05 \times 10^{-3}$	8.95 $\pm 0.12 \times 10^{-11}$	4-methyl BZ	3.65 $\pm 0.11 \times 10^{-6}$	$< 4.0 \times 10^4$
1	9.85 $\pm 0.07 \times 10^{-4}$	1.19 $\pm 0.02 \times 10^{-11}$	4-hydroxy BZ	1.55 $\pm 0.04 \times 10^{-3}$	1.31 $\pm 0.04 \times 10^8$
1	1.11 $\pm 0.00 \times 10^{-3}$	1.34 $\pm 0.02 \times 10^{-11}$	Indole	5.82 $\pm 0.05 \times 10^{-4}$	4.34 $\pm 0.01 \times 10^7$
3	2.62 $\pm 0.03 \times 10^{-3}$	3.16 $\pm 0.05 \times 10^{-11}$	Indazole	9.21 $\pm 1.95 \times 10^{-6}$	$< 3.0 \times 10^5$
3	4.15 $\pm 0.03 \times 10^{-3}$	5.00 $\pm 0.25 \times 10^{-11}$	Benzimidazole	2.88 $\pm 0.26 \times 10^{-5}$	$< 6.0 \times 10^5$

Light screening correction for organic matter solutions

Absorption spectra were recorded in 1 cm quartz cuvettes on a Cary 100 spectrophotometer (Varian) for solutions containing dissolved organic matter. The relative irradiance, I_{λ} , of the light spectrum of the Xe-lamp and the enhanced UVB light used in experimental setup were recorded with a spectrometer (OceanOptics Inc.). The screening factor, S , was determined as

$$S_{\lambda} = \frac{1 - 10^{-a_{\lambda} \cdot z}}{2.303 \cdot a_{\lambda} \cdot z}$$

with the optical density (decadic), a , at each wavelength, λ (nm), and the optical path length z (cm). The relative light intensity experienced by the test compound, I' , was estimated as follows,

$$I' = \sum_{\lambda} S_{\lambda} \times I_{\lambda,rel}$$

with the relative light intensity of the light source at each wavelength, $I_{\lambda,rel}$. The observed degradation rates of the test compounds were corrected for light screening by multiplying with a correction factor, I'^{-1} .

Table S4. Correction factors (I'^{-1}) accounting for light screening by organic matter.

material	I'^{-1}
Suwannee River Fulvic Acid (II)	
Simulated Sunlight (Xe lamp)	
13 mg _C L ⁻¹	1.11
Waskish Peat organic matter	
Enhanced UVB light	
5 mg _C L ⁻¹	1.15
10 mg _C L ⁻¹	1.33
15 mg _C L ⁻¹	1.68

References

- Arnold, W. A. (2014). "One electron oxidation potential as a predictor of rate constants of N-containing compounds with carbonate radical and triplet excited state organic matter." Environmental Science: Processes & Impacts **16**(4): 832-838.
- Brucoleri, A., B. C. Pant, et al. (1993). "Evaluation of primary photoproduct quantum yields in fulvic acid." Environmental Science & Technology **27**(5): 889-894.
- Canonica, S., B. Hellrung, et al. (2006). "Aqueous oxidation of phenylurea herbicides by triplet aromatic ketones." Environmental Science & Technology **40**(21): 6636-6641.
- Dulin, D. and T. Mill (1982). "Development and Evaluation of Sunlight Actinometers." Environmental Science & Technology **16**(11): 815-820.
- Estevao, M. S., L. C. Carvalho, et al. (2011). "Analysis of the antioxidant activity of an indole library: cyclic voltammetry versus ROS scavenging activity." Tetrahedron Letters **52**(1): 101-106.
- Hager, J. W. and S. C. Wallace (1988). "2-Laser Photoionization Supersonic Jet Mass-Spectrometry of Aromatic-Molecules." Analytical Chemistry **60**(1): 5-10.
- Zepp, R. G., P. F. Schlotzhauer, et al. (1985). "Photosensitized transformations involving electronic energy transfer in natural waters: role of humic substances." Environmental Science & Technology **19**(1): 74-81.